



Cite this: *Chem. Sci.*, 2025, **16**, 19263

All publication charges for this article have been paid for by the Royal Society of Chemistry

Received 22nd May 2025
Accepted 10th September 2025
DOI: 10.1039/d5sc03708e
rsc.li/chemical-science

Introduction

Organoboron compounds have garnered wide application in the fields of agricultural chemistry, pharmaceutical chemistry and materials science,¹ due to their good stability and versatile reactivity (e.g., Suzuki cross-coupling reactions and carbon–heteroatom bond forming reactions). Consequently, the development of C–B bond-forming reactions has long been of interest in organic synthesis.² Of the known synthetic methods for organoboron compounds, transition-metal-catalyzed boryl-functionalization of alkenes and alkynes, involving representative processes such as diboration,³ silaboration,⁴ borylstannation,⁵ cyanoboration,⁶ alkynylboration,⁷ and aminoboration,⁸ is of significant importance because it enables the simultaneous incorporation of a boron atom and other valuable functional groups into the organic molecules. In such reactions, boron reagents are usually employed to form metal–boron active intermediates, which then undergo organometallic elementary reactions to obtain the target product. Despite the above advances in this field, several limitations remain, including the troublesome handling of boron sources, metal residue in pharmaceuticals, excessive use of ligands/bases and poor functional group tolerance.^{3–8} Therefore, it is highly

desirable to address these challenges encountered in the aforementioned boryl-functionalization reactions.

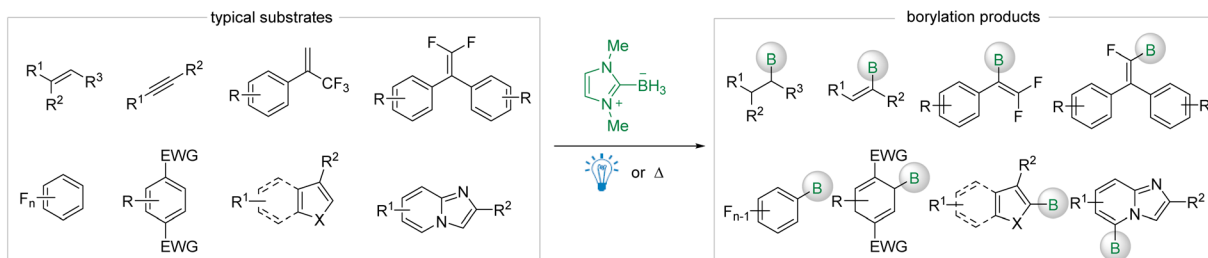
Recently, *N*-heterocyclic carbene (NHC) boranes have received increasing attention owing to their air stability and ease of handling compared to traditional boron reagents. Notably, the relatively low dissociation energies of the B–H bonds in NHC-boranes (BDE = 70–80 kcal mol^{−1}), compared to that in BH₃ (BDE = 111.7 kcal mol^{−1}), facilitate their homolysis under thermal or photoredox conditions, leading to the generation of boryl radicals.⁹ Therefore, a series of radical borylation reactions of C–C multiple bonds have been explored successively using NHC-boranes (Scheme 1a).¹⁰ To our knowledge, there are only a handful of examples of catalytic boryl-functionalization of alkenes and alkynes with NHC-boranes,^{11–14} most of which require the involvement of photocatalysts. Despite the advances in boryl-functionalization, side reactions such as hydroboration¹⁵ and radical dimerization of alkenes are often unavoidable.¹⁶ In 2020–2025, Wang¹² and Xuan¹⁴ reported visible light-induced arylboration and borylacetylation of alkenes using NHC-boranes with [Ir^{III}] as the photocatalyst (Scheme 1b). Mechanistic studies showed that a NHC-boryl radical and an arene radical anion (or a ketyl radical) are generated concurrently *via* a photoredox-catalyzed single-electron transfer (SET) process. Subsequently, the NHC-boryl radical undergoes radical addition to alkenes, followed by radical cross-coupling with the arene radical anion (or ketyl radical), affording products. Moreover, the Xie group¹³ in 2024 achieved a rare alkynylborylation reaction of alkenes with NHC-boranes and alkynyl bromides by using Ir(ppy)₂(dtbbpy)PF₆ (Scheme 1b). In this work, the authors propose that radical addition to carbon–carbon triple bonds plays a key role in the introduction of alkynyl groups. Although certain

^aKey Laboratory of Green and Precise Synthetic Chemistry and Applications, Ministry of Education, Anhui Provincial Key Laboratory of Synthetic Chemistry and Applications, College of Chemistry and Materials Science, HuaiBei Normal University, HuaiBei, Anhui 235000, P.R. China. E-mail: huangqiang9040@163.com; hongjili@chnu.edu.cn

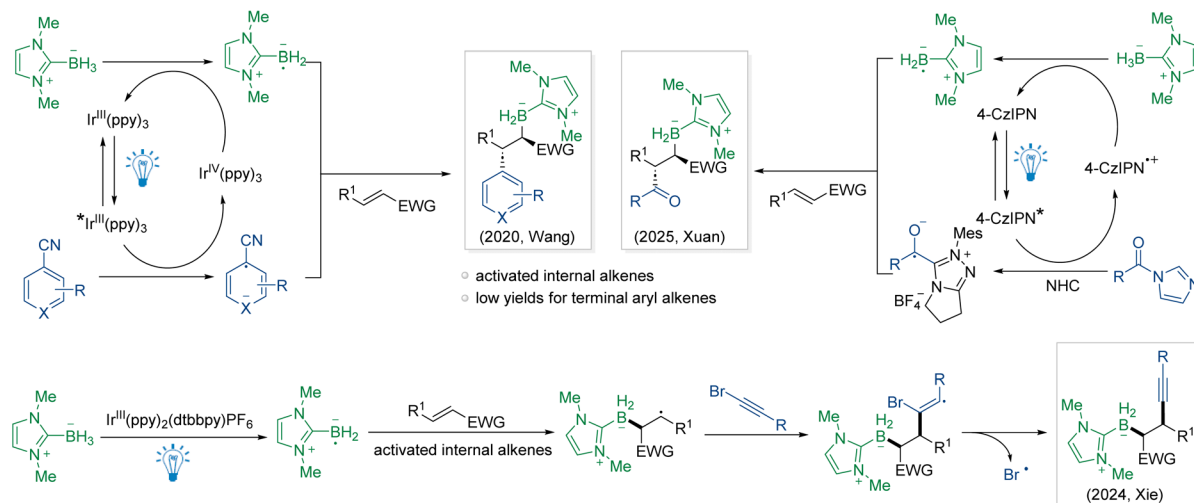
^bKey Laboratory of Advanced Drug Preparation Technologies, Ministry of Education of China, Zhengzhou University, Zhengzhou 450001, P.R. China



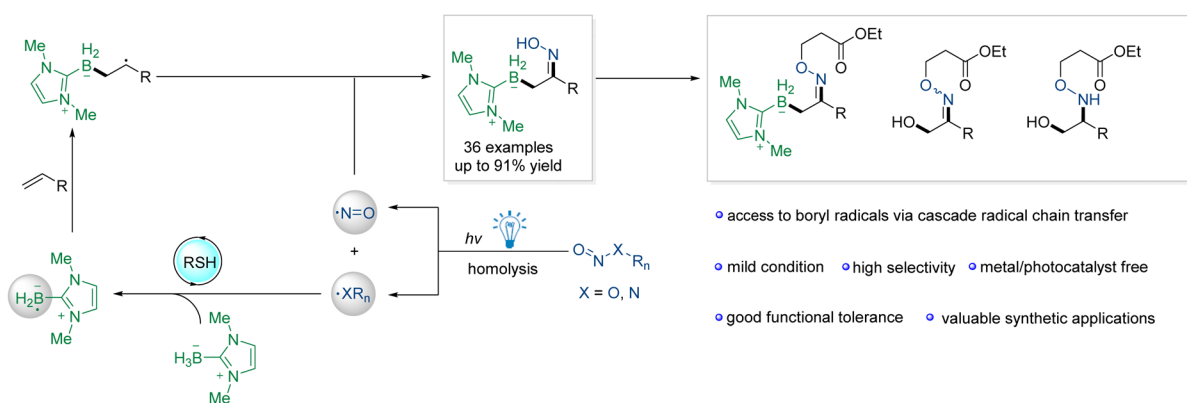
a) Radical borylation reactions of C–C multiple bonds using NHC-boranes



b) Photoredox-catalyzed radical boryl-functionalization of alkenes using NHC-boranes



c) This work: Photoinduced boryl-oximation of alkenes via NHC-boryl radical generation



Scheme 1 Strategies for the borylation/boryl-functionalization of C–C multiple bonds.

progress has been made in the boryl-functionalization of alkenes using NHC-boranes, the limited substrate scope and functional group type highlight the need for further investigation into boryl-functionalization reactions.

In recent years, significant progress has been made in the visible-light-induced radical functional-oximation of alkenes, particularly through the utilization of organonitroso compounds (BuO-NO and $\text{R}^1\text{R}^2\text{N-NO}$) as efficient NO radical sources.¹⁷ Inspired by these breakthroughs, we proposed a photoinduced cascade radical chain transfer strategy involving NHC-boranes, thiols, and nitroso compounds for the boryl-functionalization of alkenes. This approach enables the generation of boryl and NO

radicals *via* homolytic N–N/N–O bond cleavage, thereby facilitating subsequent boryl-oximation of alkenes and allowing for the efficient synthesis of functionalized organoboron compounds (Scheme 1c). Notably, the newly established boryl-oximation proceeds well in the absence of any photocatalysts and exhibits excellent functional group tolerance, broad substrate scope, and compatibility with late-stage functionalization.

Results and discussion

Initially, methyl 4-vinylbenzoate **1aa**, borane adduct **2** and *N*-nitrosopiperidine **3a** were chosen as the model substrates to



Table 1 Selected optimization results

Entry	Deviation from optimized conditions ^a	4aa ^b (yield, %)		Conv. ^b (%)
		4aa ^b (yield, %)	5aa ^b (yield, %)	
1	None	93 (88) ^c	<5	>95
2 ^d	376–400 nm LEDs	24	6	>95
3 ^d	406–443 nm LEDs	42	12	>95
4 ^d	420–480 nm LEDs	32	13	>95
5 ^d	437–471 nm LEDs	52	10	81
6 ^e	THF	56	16	>95
7 ^e	Dioxane	54	13	93
8 ^e	DMF	55	13	>95
9 ^e	EtOH	45	<5	75
10 ^e	‘PrOH	55	<5	85
11 ^e	Acetone	52	12	>95
12 ^e	DCM	43	10	87
13 ^e	Toluene	65	8	94
14	No 1,2-ethanedithiol	<5	<5	<5
15	In the dark	n.d	n.d	0
16	Air	30	7	>95

^a Reaction conditions: 1aa (0.3 mmol), 2 (0.9 mmol), 3a (0.6 mmol), 1,2-ethanedithiol (20 mol%), toluene (3.0 mL), 20 W 437–471 nm LEDs, rt, 40 h, and under N₂. ^b Determined by ¹H NMR using 1,3,5-trimethoxybenzene as an internal standard. ^c The data in parentheses are isolated yields. ^d 1aa (0.3 mmol), 2 (0.3 mmol), 3a (0.45 mmol), 1,2-ethanedithiol (20 mol%), CH₃CN (3.0 mL), rt, 30 h, and under N₂. ^e 1aa (0.3 mmol), 2 (0.3 mmol), 3a (0.45 mmol), 1,2-ethanedithiol (20 mol%), solvent (3.0 mL), 20 W 437–471 nm LEDs, rt, 30 h, and under N₂.

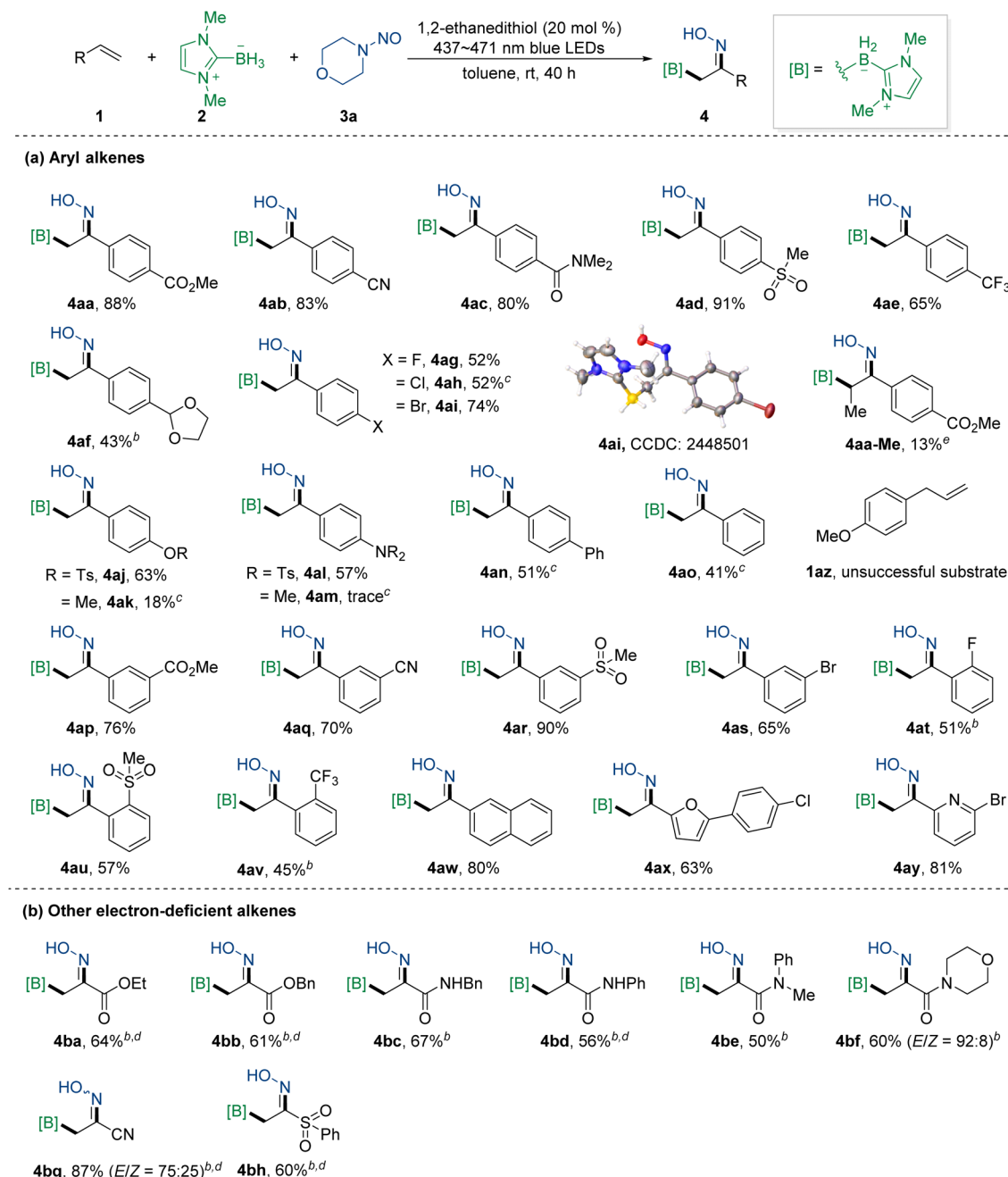
optimize the reaction conditions, and the results are listed in Table 1. After the systematic screening, the best reaction conditions were obtained as follows: 1aa (1.0 equiv.), 2 (3.0 equiv.), 3a (2.0 equiv.), and 1,2-ethanedithiol (20 mol%) in a solution of toluene at room temperature under blue LED (20 W, 437–471 nm) irradiation for 40 h, producing the desired product 4aa in 88% isolated yield (entry 1). The observed stereoselectivity is further supported by the single-crystal structure of the product 4ai (CCDC number: 2448501).¹⁸ In addition, the wavelength of the light source significantly influences the reactivity and selectivity of the model reaction. Remarkably, the screening of light sources showed that the use of 437–471 nm LEDs resulted in the formation of 4aa in 52% yield and 81% conv. (entries 2–5).

Interestingly, during the course of optimization, a byproduct 5aa was isolated and well characterized (also see Scheme 3d). We further found that the choice of solvent significantly influenced the reaction efficiency. Under irradiation with blue LEDs (20 W, 437–471 nm), most solvents afforded product 4aa in approximately 50% yield, while toluene serving as the optimal solvent enhanced the yield to 65% (entries 6–13). Control experiments showed that the reaction almost could not proceed in the absence of the thiol catalyst or light irradiation (entries 14–15). The reaction proceeded under ambient air, however, the 4aa was achieved with only 30% isolated yield (entry 16). We next focused on evaluating some other reaction parameters (see Table S1 for details). Thiol catalysts with different substituents afforded product 4aa with comparable yields, while using

thiophenol as a catalyst only resulted in a 10% yield. Alkyl-substituted nitrosamines showed favorable results for the formation of the main product, whereas aryl-substituted nitrosamines and ‘BuONO (TBN) provided lower yields. Finally, the yield could be further improved by adjusting the material ratio to an excessive amount of 2 and 3a.

Subsequently, we investigated the substrate scope under the optimal conditions listed in Table 1 (Table 2). First, we studied the substituent effect on the aromatic rings of styrene derivatives. The reaction demonstrated good functional group compatibility, tolerating a variety of substituents, including ester, cyano, acylamino, sulfonyl, trifluoromethyl, acetal, and halogen groups. Most of the arylalkenes with an electron-withdrawing group at the *para*-position afforded boryloximation products (4aa–4ae, 4ag–4aj, and 4al) in moderate to excellent yields (52–91%). Individually, the reaction of 2-(4-vinylphenyl)-1,3-dioxolane was sluggish, affording the desired product 4af only in 43% yield. Notably, when PhCN was used as the solvent instead of PhMe, both 4-phenylstyrene and styrene participated in the reaction, affording the corresponding products 4an and 4ao in 51% and 41% yields, respectively. Styrenes with electron-donating groups and internal olefins exhibited relatively poor reactivity. As a result, 4-(dimethylamino)styrene, 4-methoxystyrene and methyl-4-(prop-1-en-1-yl)benzoate yielded the corresponding products (4ak, 4am, and 4aa-Me) only in trace to 18% yields, with most of the alkene substrates remaining unreacted.



Table 2 Photoinduced boryl-oximation of alkenes: substrate scope^{a,b,c,d,e}

^a Unless otherwise noted, the reaction conditions were the same as those described in Table 1, entry 1, 1 (0.5 mmol), 2 (1.5 mmol), 3a (1.0 mmol), 1,2-ethanedithiol (20 mol%), toluene (5.0 mL), 20 W 437–471 nm LEDs, rt, 40 h, and under N₂. The isomer ratios were determined by ¹H NMR.

^b Used ³BuSH (50 mol%) as the catalyst. ^c Used PhCN (5.0 mL) as the solvent. ^d Used ³BuONO (TBN, 1.0 mmol) as the NO radical source. ^e 1 (1.0 mmol), 2 (3.0 mmol), 3a (2.0 mmol), 1,2-ethanedithiol (20 mol%), PhCN (5.0 mL), 20 W 437–471 nm LEDs, rt, 40 h, and under N₂.

We next found that *meta*-substituted substrates delivered the desired products in good yields (4ap–4as, 65–90%), whereas *ortho*-substituted counterparts showed reduced reactivity (4at–4av, 45–57%), indicating a mild steric effect in the boryl-oximation of alkenes. In addition to styrene and its derivatives, a fused-ring-substituted ethylene (*i.e.*, 2-naphthyl ethylene, corresponding to 4aw, 80%) and furanyl and pyridyl

ethylenes (corresponding to 4ax–4ay, 63–81%) could also provide favorable results. Subsequently, we randomly evaluated the applicability of an aliphatic olefin 1az in this reaction. Unfortunately, 1az did not react with 2 and 3a under the standard conditions, and no desired product was observed. Remarkably, by fine-tuning the standard conditions (using ³BuONO instead of 3a or employing 50 mol% ³BuSH as

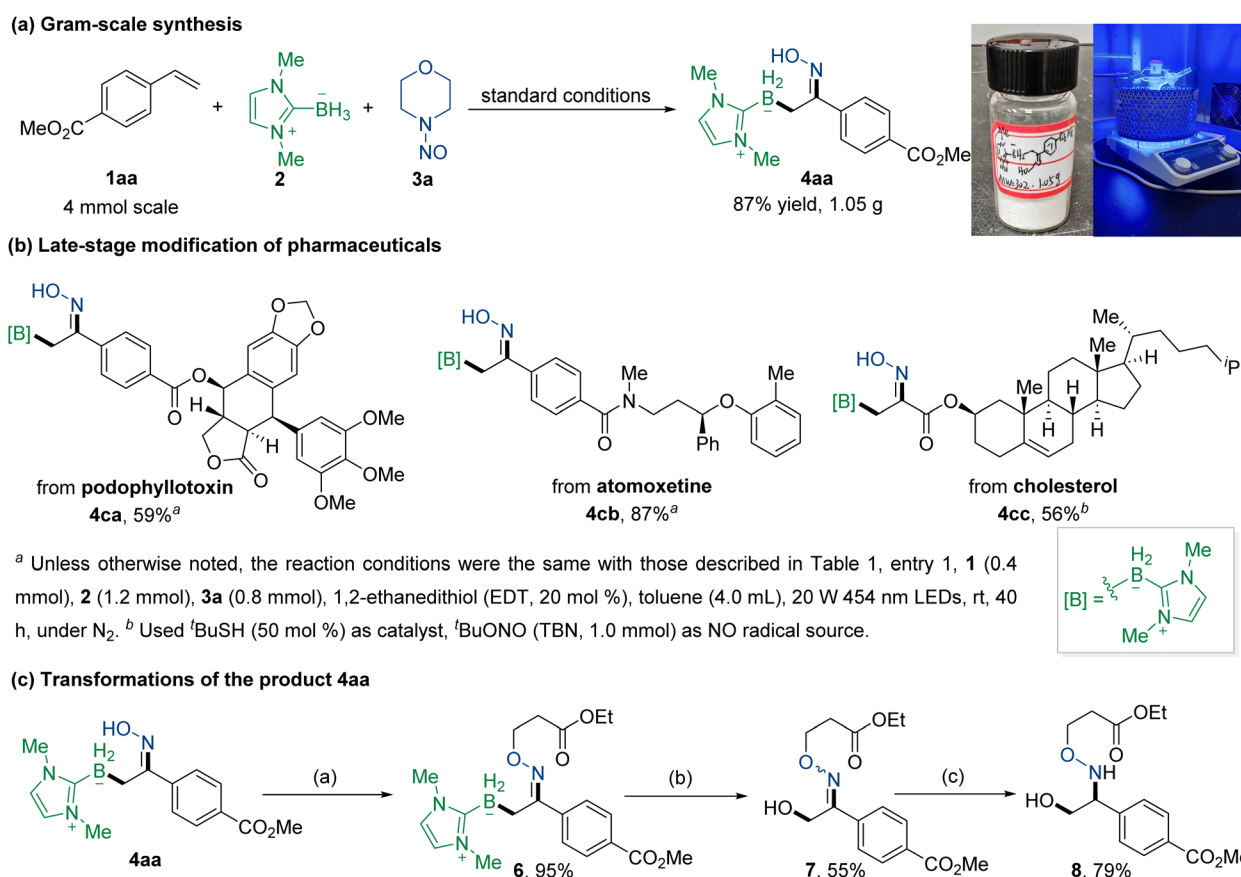


a catalyst), the reaction could be further extended to functionalized alkenes including ester-, amide-, cyano- and sulfonyl-substituted ethylenes. Specifically, ethyl acrylate, benzyl acrylate, and phenyl vinyl sulfone gave the corresponding products (**4ba**–**4bb** and **4bh**) in moderate yields with high selectivities. *N*-substituted acrylamides bearing phenyl, benzyl or alkyl reacted smoothly to afford **4bc**–**4bf** in moderate yields. Finally, acrylonitrile demonstrated excellent reactivity, delivering the boryl-oximation product **4bg** in 87% yield, albeit with relatively lower stereoselectivity.

Subsequently, we demonstrated the practicality of this method through gram-scale synthesis and late-stage functionalization of bioactive molecules. First, the model reaction was readily scaled up to a gram scale, affording compound **4aa** with well retained yield (Scheme 2a, 87% yield, 1.05 g of product **4aa** was obtained). Next, we evaluated the applicability of this protocol to the late-stage modification of multifunctionalized alkene-containing pharmaceutical derivatives (Scheme 2b). The results showed that derivatives of podophyllotoxin, atomoxetine, and cholesterol proceeded well to afford boryl-oximation products **4ca**–**4cc** in 56–87% yields. Given the widespread presence of oxime ether scaffolds in pharmaceuticals¹⁹—which demonstrate diverse biological activities such as

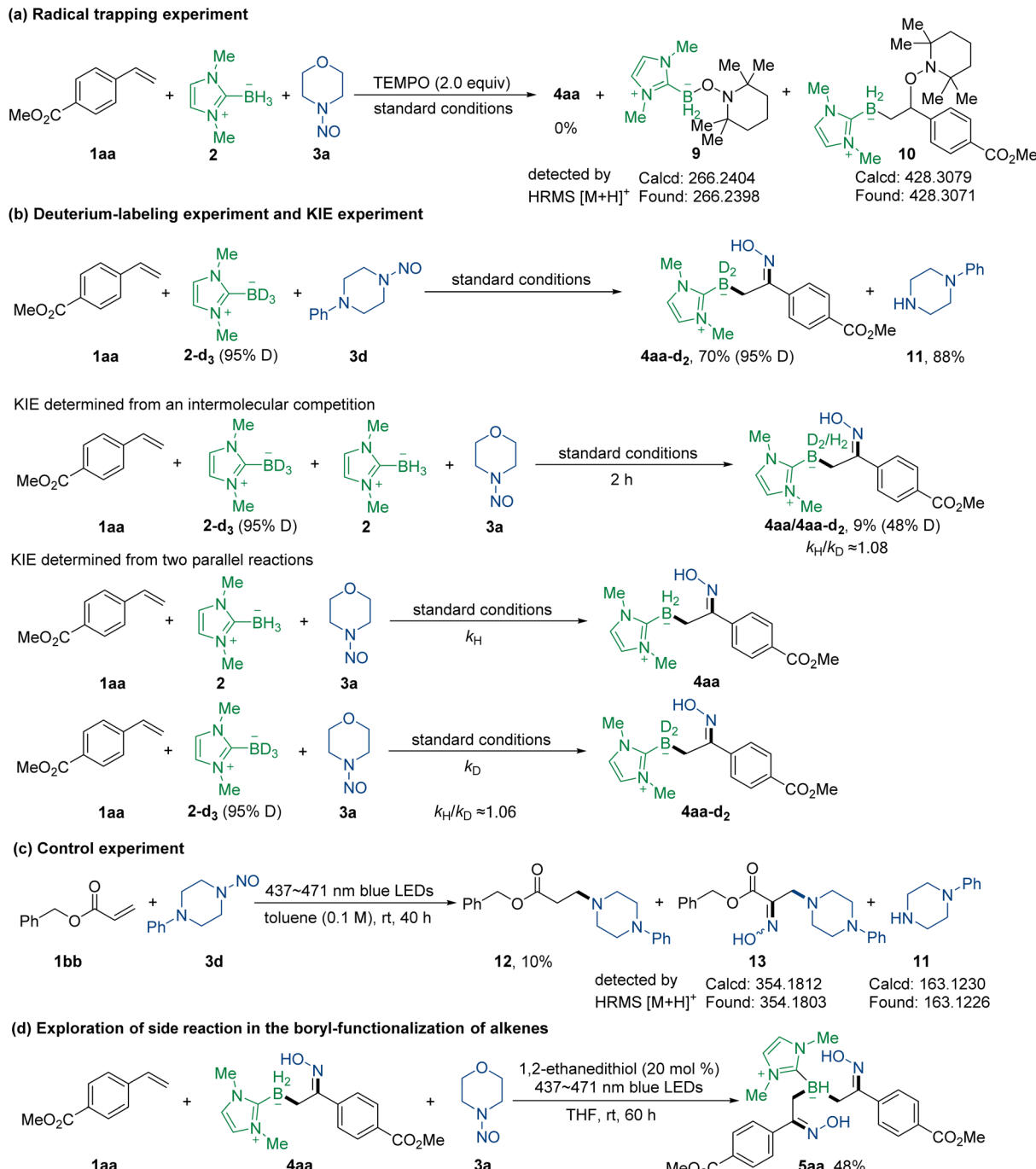
antifungal, antibacterial, antiviral and antidepressive effects—along with their versatile reactivity in synthetic chemistry,²⁰ we further explored the transformation of product **4aa** (Scheme 2c). Specifically, **4aa** could smoothly undergo a Michael addition with ethyl acrylate using triphenylphosphine as a catalyst,²¹ leading to the formation of α -boryl oxime ether **6** in 95% yield with retention of configuration. The oxidative cleavage of the C–B bond in **6** yielded α -hydroxy oxime ether **7**, which was further reduced with NaCNBH₃ to afford amino alcohol **8** in 79% yield.

To understand the possible reaction mechanism, several control experiments were designed and conducted (Scheme 3). A radical-trapping experiment was performed by adding the radical scavenger TEMPO to the reaction system (Scheme 3a). The experimental results revealed that no target **4aa** was formed, but both the adducts **9** and **10** were detected by high-resolution mass spectrometry, indicating that boryl radicals were involved therein. In addition, the absorption of **1aa**, **2** and **3a** (ranging from 380 to 440 nm) was clearly observed with UV-vis absorbance, showing that the peaks of **3a** are mainly located near the UV region (see Fig. S5 for details). Next, a deuterium labeling experiment with the reaction of **1aa**, **2-d₃** and **3d** was carried out under the standard conditions (Scheme 3b). We found that the deuteration rate of the product **4aa-d₂** was



Scheme 2 Applications of the boryl-oximation protocol and transformations of the products.



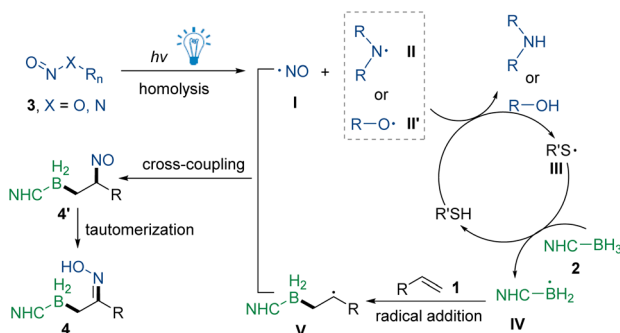


Scheme 3 Mechanistic studies.

consistent with that of the borane adduct **2-d₃**, indicating that the B–D bonds in both the reactant and product did not undergo H–D exchange during the reaction. Notably, 1-phenylpiperazine **11** was also obtained in 88% yield, which provides further evidence for the proposed reaction mechanism. Subsequently, the kinetic isotope effect (KIE) value of borane was determined through an intermolecular competition and two parallel reactions, with both results being close to 1.0. These experimental results suggest that the generation of boryl radicals might not be the rate-determining step (Scheme 3b). To

further corroborate the homolytic cleavage mechanism of *N*-nitrosamine, a control experiment was conducted in the absence of compound **2** (Scheme 3c). The reaction of benzyl acrylate (**1bb**) with 1-nitroso-4-phenylpiperazine (**3d**) afforded the hydroamination product **12** in 10% yield. Trace amounts of the aminooximation product **13** and 1-phenylpiperazine **11** were also detected by high-resolution mass spectrometry. These results further support that *N*-nitrosamine generates amino and nitrosyl radicals upon photoirradiation. Finally, we explored the origin of the byproduct **5aa** observed in the reaction (Scheme





Scheme 4 Proposed mechanism.

3d). Experiments showed that the photoinduced secondary boryl-oximation reaction of **1aa** with **4aa** and **3a** smoothly occurred to generate the byproduct **5aa** in 48% yield. This unexpected discovery provides new access to realizing multi-functionalization of NHC-boranes.^{15h}

Based on the above control experiments and related reports,^{17,22} a plausible reaction mechanism for this boryl-functionalization of alkenes is proposed and listed in Scheme 4. First, the nitroso compound undergoes homolytic cleavage to form nitroso radical **I** and amino radical **II** (or alkoxyl radical **II'**) upon light irradiation. Subsequently, the amino radical (or alkoxyl radical) undergoes a cascade radical chain transfer process (two-step HAT) to generate the NHC-boryl radical **IV**. Moreover, light on-off experiments (see Fig. S10 for details) demonstrated that the radical chain transfer process is transient and persistent irradiation is essential to run these cascades. Next, the NHC-boryl radical undergoes addition to the alkene, generating radical intermediate **V**, which subsequently couples with the nitroso radical **I** to form the unstable intermediate **4'**. This intermediate then undergoes rearrangement to furnish the target product **4**.

Conclusions

In summary, we have developed a new method that does not rely on the use of transition metals or tailored photocatalysts for the boryl-oximation of alkenes, affording a number of useful α -boryl oxime compounds in moderate to good yields. Both the late-stage modification of various pharmaceutical molecules and the product transformations demonstrate its synthetic applications in the field of synthetic chemistry. Mechanistic experiments including radical-trapping experiments, deuterium-labeling experiments and KIE experiments disclose the possible pathway for this boryl-oximation of alkenes, in which a radical chain transfer is key for the generation of the boryl radical. The photoinduced activation mode of NHC-boranes offers an ideal platform for the bifunctionalization of alkenes. Our laboratory will focus on expanding this boryl radical-based strategy to address more challenging chemical transformations.

Author contributions

Qiang Huang (investigation, methodology, funding acquisition, and writing – original draft); Na Li (investigation and

methodology); Panke Zhang (supervision and funding acquisition); Hongji Li (conceptualization, supervision, funding acquisition, and writing – review & editing).

Conflicts of interest

The authors declare no competing financial interest.

Data availability

CCDC 2448501 contains the supplementary crystallographic data for this paper.²³

The detailed experimental process and additional data associated with this work are available in the SI. See DOI: <https://doi.org/10.1039/d5sc03708e>.

Acknowledgements

We gratefully acknowledge financial support from the National Natural Science Foundation of China (22401103), the Scientific Research Projects of Higher Education Institutions in Anhui Province (2024AH051684); the Open Project of Key Laboratory of Advanced Drug Preparation Technologies, Ministry of Education of China (ZKF202403); the Anhui Province Research Funding for Outstanding Young Talents in Colleges and Universities, China (No. 2022AH020039).

Notes and references

- For selected reviews, see: (a) A. Suzuki, *Angew. Chem., Int. Ed.*, 2011, **50**, 6722–6737; (b) R. Jana, T. P. Pathak and M. S. Sigman, *Chem. Rev.*, 2011, **111**, 1417–1492; (c) L. Xu, S. Zhang and P. Li, *Chem. Soc. Rev.*, 2015, **44**, 8848–8858; (d) B. S. L. Collins, C. M. Wilson, E. L. Myers and V. K. Aggarwal, *Angew. Chem., Int. Ed.*, 2017, **56**, 11700–11733.
- For selected reviews, see: (a) H. C. Brown and B. Singaram, *Acc. Chem. Res.*, 1988, **21**, 287–293; (b) K. Burgess and M. J. Ohlmeyer, *Chem. Rev.*, 1991, **91**, 1179–1191; (c) J. Chen, J. Guo and Z. Lu, *Chin. J. Chem.*, 2018, **36**, 1075–1109.
- For selected examples: (a) J. B. Morgan, S. P. Miller and J. P. Morken, *J. Am. Chem. Soc.*, 2003, **125**, 8702–8703; (b) N. F. Pelz, A. R. Woodward, H. E. Burks, J. D. Sieber and J. P. Morken, *J. Am. Chem. Soc.*, 2004, **126**, 16328–16329; (c) J. Ramírez, R. Corberán, M. Sanaú, E. Peris and E. Fernandez, *Chem. Commun.*, 2005, 3056–3058; (d) H. E. Burks, S. Liu and J. P. Morken, *J. Am. Chem. Soc.*, 2007, **129**, 8766–8773; (e) H. E. Burks, L. T. Kliman and J. P. Morken, *J. Am. Chem. Soc.*, 2009, **131**, 9134–9135; (f) L. T. Kliman, S. N. Mlynarski and J. P. Morken, *J. Am. Chem. Soc.*, 2009, **131**, 13210–13211; (g) H. Yoshida, S. Kawashima, Y. Takemoto, K. Okada, J. Ohshita and K. Takaki, *Angew. Chem., Int. Ed.*, 2012, **51**, 235–238.
- For selected examples: (a) T. Ohmura, H. Taniguchi, Y. Kondo and M. Sugino, *J. Am. Chem. Soc.*, 2007, **129**, 3518–3519; (b) T. Ohmura, K. Matsuda and M. Sugino, *J. Am. Chem. Soc.*, 2008, **130**, 1526–1527; (c) M. Zhao,



C.-C. Shan, Z.-L. Wang, C. Yang, Y. Fu and Y.-H. Xu, *Org. Lett.*, 2019, **21**, 6016–6020.

5 S.-Y. Onozawa, Y. Hatanaka, T. Sakakura, S. Shimada and M. Tanaka, *Organometallics*, 1996, **15**, 5450–5452.

6 (a) M. Suginome, A. Yamamoto and M. Murakami, *J. Am. Chem. Soc.*, 2003, **125**, 6358–6359; (b) M. Suginome, A. Yamamoto and M. Murakami, *Angew. Chem., Int. Ed.*, 2005, **44**, 2380–2382; (c) M. Suginome, A. Yamamoto, T. Sasaki and M. Murakami, *Organometallics*, 2006, **25**, 2911–2913; (d) A. Yamamoto, Y. Ikeda and M. Suginome, *Tetrahedron Lett.*, 2009, **50**, 3168–3170.

7 M. Suginome, M. Shirakura and A. Yamamoto, *J. Am. Chem. Soc.*, 2006, **128**, 14438–14439.

8 (a) N. Matsuda, K. Hirano, T. Satoh and M. Miura, *J. Am. Chem. Soc.*, 2013, **135**, 4934–4937; (b) R. Sakae, K. Hirano and M. Miura, *J. Am. Chem. Soc.*, 2015, **137**, 6460–6463; (c) J. Huo, Y. Xue and J. Wang, *Chem. Commun.*, 2018, **54**, 12266–12269; (d) Y. Zhang and X.-F. Wu, *Org. Chem. Front.*, 2020, **7**, 3382–3386.

9 (a) S.-H. Ueng, M. M. Brahmi, É. Derat, L. Fensterbank, E. Lacôte, M. Malacria and D. P. Curran, *J. Am. Chem. Soc.*, 2008, **130**, 10082–10083; (b) D. P. Curran, A. Solovyev, M. M. Brahmi, L. Fensterbank, M. Malacria and E. Lacôte, *Angew. Chem., Int. Ed.*, 2011, **50**, 10294–10317; (c) M.-A. Tehfe, J. Monot, M. Malacria, L. Fensterbank, J.-P. Fouassier, D. P. Curran, E. Lacôte and J. Lalevée, *ACS Macro Lett.*, 2012, **1**, 92–95.

10 For selected reviews: (a) F. W. Friese and A. Studer, *Chem. Sci.*, 2019, **10**, 8503–8518; (b) T. Taniguchi, *Eur. J. Org. Chem.*, 2019, **2019**, 6308–6319; (c) J. Jin, H. Xia, F. Zhang and Y. Wang, *Chin. J. Org. Chem.*, 2020, **40**, 2185–2194; (d) X. Chen, X. Zhou, J. He and X. Liu, *Synthesis*, 2025, **57**, 2539–2550.

11 (a) M. Shimoi, K. Maeda, S. J. Geib, D. P. Curran and T. Taniguchi, *Angew. Chem., Int. Ed.*, 2019, **58**, 6357–6361; (b) H. Ni, Y. Li, C. Li and Z. Liu, *RSC Adv.*, 2025, **15**, 4652–4656.

12 J. Qi, F.-L. Zhang, J.-K. Jin, Q. Zhao, B. Li, L.-X. Liu and Y.-F. Wang, *Angew. Chem., Int. Ed.*, 2020, **59**, 12876–12884.

13 C. Zhu, S. Yao and J. Xie, *Synthesis*, 2024, **56**, 1711–1718.

14 Z.-L. Chen, S.-C. Ma, S.-Y. Tang, H.-Y. Yu, Y. Zhao and J. Xuan, *ACS Catal.*, 2025, **15**, 7101–7111.

15 For selected examples: (a) T. Watanabe, D. Hirose, D. P. Curran and T. Taniguchi, *Chem.-Eur. J.*, 2017, **23**, 5404–5409; (b) S.-C. Ren, F.-L. Zhang, J. Qi, Y.-S. Huang, A.-Q. Xu, H.-Y. Yan and Y.-F. Wang, *J. Am. Chem. Soc.*, 2017, **139**, 6050–6053; (c) M. Shimoi, T. Watanabe, K. Maeda, D. P. Curran and T. Taniguchi, *Angew. Chem., Int. Ed.*, 2018, **57**, 9485–9490; (d) N. Zhou, X.-A. Yuan, Y. Zhao, J. Xie and C. Zhu, *Angew. Chem., Int. Ed.*, 2018, **57**, 3990–3994; (e) P.-J. Xia, D. Song, Z.-D. Ye, Y.-Z. Hu, J.-A. Xiao, H.-Y. Xiang, X.-Q. Chen and H. Yang, *Angew. Chem., Int. Ed.*, 2020, **59**, 6706–6710; (f) C. Zhu, J. Dong, X. Liu, L. Gao, Y. Zhao, J. Xie, S. Li and C. Zhu, *Angew. Chem., Int. Ed.*, 2020, **59**, 12817–12821; (g) F. Xie, Z. Mao, D. P. Curran, H. Liang and W. Dai, *Angew. Chem., Int. Ed.*, 2023, **62**, e202306846; (h) F.-X. Li, X. Wang, J. Lin, X. Lou, J. Ouyang, G. Hu and Y. Quan, *Chem. Sci.*, 2023, **14**, 6341–6347.

16 M. Golfmann, L. Glagow, A. Giakoumidakis, C. Golz and J. C. L. Walker, *Chem.-Eur. J.*, 2023, **29**, e202202373.

17 (a) D. V. Patil, T. Si, H. Y. Kim and K. Oh, *Org. Lett.*, 2021, **23**, 3105–3109; (b) S. Plöger and A. Studer, *Org. Lett.*, 2022, **24**, 8568–8572; (c) Z. Wang, N. Wierich, J. Zhang, C. G. Daniliuc and A. Studer, *J. Am. Chem. Soc.*, 2023, **145**, 8770–8775; (d) H. Lan, Y. Su, Y. Chen, X. He and D. Wang, *Org. Chem. Front.*, 2024, **11**, 4207–4213; (e) W. Li, C. Diao, Y. Lu and H. Li, *Org. Lett.*, 2024, **26**, 6253–6258.

18 CCDC number: 2448501 for **4ai**; the regarding crystallographic data can be obtained from the Cambridge Crystallographic Data Centre. Website: <https://www.ccdc.cam.ac.uk>.

19 (a) A. D. Latif, T. Gonda, M. Vágvölgyi, N. Kúsz, Á. Kulmány, I. Ocsovszki, Z. P. Zomborszki, I. Zupkó and A. Hunyadi, *Int. J. Mol. Sci.*, 2019, **20**, 2184; (b) T. Kosmalski, D. Kupczyk, S. Baumgart, R. Paprocka and R. Studzińska, *Molecules*, 2023, **28**, 5041.

20 (a) M. Ueda, *Chem. Pharm. Bull.*, 2014, **62**, 845–855; (b) J. Li, Y. Hu, D. Zhang, Q. Liu, Y. Dong and H. Liu, *Adv. Synth. Catal.*, 2017, **359**, 710–771; (c) X.-Y. Yu, J.-R. Chen and W.-J. Xiao, *Chem. Rev.*, 2021, **121**, 506–561; (d) B. Lu, J. Yu, X. Zhang and G. Chen, *Tetrahedron Lett.*, 2024, **136**, 154914.

21 D. Bhuniya, S. Mohan and S. Narayanan, *Synthesis*, 2003, 1018.

22 X. Pan, E. Lacôte, J. Lalevée and D. P. Curran, *J. Am. Chem. Soc.*, 2012, **134**, 5669–5674.

23 Q. Huang, N. Li, P. Zhang and H. Li, CCDC 2448501: Experimental Crystal Structure Determination, 2025, DOI: [10.5517/ccdc.csd.cc2n5vxm](https://doi.org/10.5517/ccdc.csd.cc2n5vxm).

